Perfect coherent shift of bound pairs in strongly correlated systems

L. Jin and Z. Song*
School of Physics, Nankai University, Tianjin 300071, China
(Received 1 June 2010; revised manuscript received 31 March 2011; published 3 May 2011)

In the present work we extend the concept of coherent shift for the extended Bose-Hubbard model and Fermi-Hubbard model. We present two types of local bound pairs (BPs) for the Bose system and one type for the Fermi system. It is shown exactly that the perfect coherent shift can be achieved in such models in the large binding-energy limit. We find that for a Bose on-site BP, the perfect coherent shift condition depends on the nearest-neighbor interaction strength and the momentum of the incident single-particle wave packet, while for the other two types of BPs, it is independent of the initial state in the proposed systems. Numerical simulation of the scattering process between a single particle and a BP in a finite-size system is conducted and the computational results are shown to confirm the analytical investigation.

DOI: 10.1103/PhysRevA.83.052102 PACS number(s): 03.65.Ge, 03.67.Lx, 05.30.Jp, 03.65.Nk

I. INTRODUCTION

The bound pair (BP) state and its dynamics are interesting recent topics in quantum physics and quantum information [1–11]. In a previous work [10], we studied the dynamics of a BP and the interaction between a single particle and a BP in a simple Bose-Hubbard model with an on-site coupling strength U and nearest-neighbor hopping κ. Within the large U regime, we found an interesting scattering process, coherent shift, between them. A BP is formed by two particles occupying a single site, which is stable when the binding energy is large enough. It acts as a single particle with a hopping strength $2\kappa^2/U$. When a moving particle encounters a BP, they will switch their roles by transferring a particle from a doubly occupied state to a singly occupied state with amplitude 2κ. During this process, the BP acquires a one-spacing shift in the case of $2\kappa \gg 2\kappa^2/U$, i.e., the jump of the BP induced by the collision is very much faster than its spontaneous hopping. We believed that this phenomenon should not be exclusive and could be applied to quantum device designs. In addition, Valiente *et al.* performed a comprehensive numerical simulation of such a scattering process, which is useful to understand this phenomenon [12]. It was pointed that a perfect coherent shift is hardly realized in such a uniform Bose-Hubbard system. The imperfect transmission may due to the difference between the BP shift amplitude 2κ and the single-particle hopping strength κ in a simplest *uniform* Bose-Hubbard chain. Although a perfect coherent shift can be achieved in the deliberately designed chain [10], the inhomogeneity of such a system will be an obstacle to realize the perfect coherent shift in a many-particle system.

In this paper, we present three examples to demonstrate how to realize the perfect coherent shift in both boson and fermion systems in a uniform manner. We present two types of local BPs for the Bose system and one type for the Fermi system. It is shown exactly that the perfect coherent shift can be achieved in such models. We find that for a Bose on-site BP, the perfect coherent shift condition depends on the nearest-neighbor (NN) interaction strength and the momentum of the incident single-particle wave packet, while for the other two types of BPs, it is independent of the initial state in the proposed systems. In order to verify the analytical result, a numerical simulation of the scattering process between a single particle and a BP in a finite-size system is conducted. Our results indicate that the perfect coherent shift can be achieved and has great potential for future applications.

The paper is organized as follows: In Sec. II, we introduce an extended Bose-Hubbard model and the formation of the two-particle bound state. In Sec. III, we investigate the coherent shift process for an on-site BP in the case of weak NN interaction. Section IV is devoted to the same discussion for the NN BP. In Sec. V, we introduce the on-site BP in the Fermi system and demonstrate how to perform a perfect coherent shift. Section VI is devoted to the conclusion and a short discussion.

II. EXTENDED BOSE-HUBBARD MODEL

We begin with the Bose on-site BP, considering the scattering process between it and a single boson in an extended Bose-Hubbard model. The Hamiltonian reads

$$H^{\mathrm{B}} = -\kappa \sum_i (a_i^\dagger a_{i+1} + \mathrm{H.c.}) + \frac{U}{2}\sum_i n_i(n_i - 1) + V\sum_i n_i n_{i+1}, \qquad (1)$$

where $a_i^\dagger$ (a_i) is the particle creation (annihilation) operator and $n_i = a_i^\dagger a_i$ is the number operator at the ith lattice site. The tunneling strength and the on-site interaction between bosons are denoted by κ and U. We consider an odd-site system with $N = 2N_0 + 1$, with periodic boundary conditions $a_{N+1} = a_1$. The Hamiltonian of Eq. (1) has an additional NN interaction V in comparison to the Hamiltonian of Eq. (1) in the previous paper [10].

First, a state in two-particle Hilbert space, as shown in Ref. [10], can be written as

$$|\psi_k\rangle = \sum_r f^k(r)|\phi_r^k\rangle, \qquad (2)$$

*songtc@nankai.edu.cn

with

$$|\phi_0^k\rangle = \frac{1}{\sqrt{2N}} \sum_j e^{ikj} a_j^{\dagger 2} |\text{vac}\rangle,$$
$$|\phi_r^k\rangle = \frac{1}{\sqrt{N}} e^{ikr/2} \sum_j e^{ikj} a_j^{\dagger} a_{j+r}^{\dagger} |\text{vac}\rangle. \tag{3}$$

Here $|\text{vac}\rangle$ is the vacuum state for the boson operator a_i. $k = 2\pi n/N$, $n \in [1,N]$ denotes the momentum with $N = 2N_0 + 1$, and $r \in [1,N_0]$ is the distance between the two particles. The matrix representation for the Hamiltonian operator H^{B} in the basis $\{|\phi_j^k\rangle\}$ is

$$H^k = \begin{pmatrix} U & \sqrt{2}T^k & & & \\ \sqrt{2}T^k & V & T^k & & \\ & T^k & & \ddots & \\ & & \ddots & & T^k \\ & & & T^k & T^k_{N_0} \end{pmatrix}, \tag{4}$$

where $T^k = -2\kappa \cos(k/2)$, and $T^k_{N_0} = (-1)^n T^k$. Note that for an arbitrary k, the eigenvalues of Eq. (4) are equivalent to that of the single-particle $(N_0 + 1)$-site tight-binding chain system with one abnormal NN hopping amplitude $\sqrt{2}T^k$ between the zeroth ($|\phi_0^k\rangle$) and the first site ($|\phi_1^k\rangle$), and the on-site potentials U, V, and $T^k_{N_0}$ at the zeroth, first, and N_0-th sites, respectively. It follows that in each k-invariant subspace, there are three types of bound states arising from the on-site potentials under the following conditions. In the case with $|U - V| \gg |\kappa|$, the particle can be localized at either the zeroth or the first site, corresponding to (i) the on-site BP state or (ii) the NN BP state. Interestingly, in the case of $U = V$, and $|U|,|V| \gg |\kappa|$, the particle can be in the bonding state (or antibonding state) between the zeroth and the first sites, which was discussed in Ref. [13]. In previous works [10,11], the bound states of (i) and (ii) were well investigated. In Ref. [10], it was shown that the coherent shift of an on-site BP occurs when a single particle meets it. In the following we focus on the scattering process between a BP and a single particle in the presence of NN interaction. We will show exactly that the NN interaction can lead to a perfect coherent shift.

III. ON-SITE BOUND PAIR IN BOSE SYSTEM

Now we start with the on-site BP state. The formation of the BP state in the Bose-Hubbard system was studied in Refs. [1,9–11]. Here in the extended Bose-Hubbard model, the on-site BP corresponds to the BP bounded by U in the case of large U but weak V, with $|U| \gg |\kappa| \sim |V|$. In this case, the solution of $f^k(r)$ has the form

$$f^k(r) \simeq \begin{cases} 1 & (r = 0), \\ 0 & (r \neq 0), \end{cases} \tag{5}$$

with eigenenergy

$$\varepsilon_k \simeq U + \frac{4\kappa^2}{U}(\cos k + 1). \tag{6}$$

One can see that the on-site BP state acts as a composite particle with an effective hopping strength of $2\kappa^2/U$. According to Ref. [12], the effective Hamiltonian for a single on-site BP and a single particle in the extended Bose-Hubbard system can be obtained in the form

$$\begin{aligned} H_{\text{eff}}^{\text{U}} = {} & -\kappa \sum_i (\tilde{a}_i^\dagger \tilde{a}_{i+1} + 2\tilde{b}_{i+1}^\dagger \tilde{b}_i \tilde{a}_i^\dagger \tilde{a}_{i+1} + \text{H.c.}) \\ & + \frac{2\kappa^2}{U} \sum_i (\tilde{b}_i^\dagger \tilde{b}_{i+1} + \text{H.c.}) + \left(2V - \frac{7\kappa^2}{2U}\right) \\ & \times \sum_i \tilde{b}_i^\dagger \tilde{b}_i (\tilde{a}_{i-1}^\dagger \tilde{a}_{i-1} + \tilde{a}_{i+1}^\dagger \tilde{a}_{i+1}) \\ & + \left(U + \frac{4\kappa^2}{U}\right) \sum_i \tilde{b}_i^\dagger \tilde{b}_i, \end{aligned} \tag{7}$$

where $\tilde{a}_i$ and $\tilde{b}_i$ denote the hardcore bosons satisfying the following commutation relations: $[\tilde{a}_j,\tilde{a}_i^\dagger] = [\tilde{b}_j,\tilde{a}_i^\dagger] = [\tilde{b}_j,\tilde{b}_i^\dagger] = 0$, $(i \neq j)$; $\{\tilde{a}_i,\tilde{a}_i^\dagger\} = \{\tilde{b}_i,\tilde{b}_i^\dagger\} = 1$; $\{\tilde{b}_i,\tilde{a}_i^\dagger\} = \{\tilde{b}_i,\tilde{a}_i\} = 0$. The former two terms of $H_{\text{eff}}^{\text{U}}$ depict the hoppings while the last two terms depict the interaction between the two kinds of particles. The term $\tilde{b}_{i+1}^\dagger \tilde{b}_i \tilde{a}_i^\dagger \tilde{a}_{i+1}$ represents the swapping between the BP and the single particle and the term $\tilde{b}_i^\dagger \tilde{b}_i (\tilde{a}_{i-1}^\dagger \tilde{a}_{i-1} + \tilde{a}_{i+1}^\dagger \tilde{a}_{i+1})$ is NN interaction. In the case of $V = 0$, $H_{\text{eff}}^{\text{U}}$ reduces to the effective Hamiltonian presented in Ref. [12]. As pointed by Ref. [12], these terms act as the barriers to an incident single-particle wave packet, which leads to irreversible reflection. At the region around $|U/\kappa| = 10$, as shown in Fig. 1 of Ref. [12], $7\kappa^2/2U$ cannot be neglected and plays an important role in the scattering process. Furthermore, even in the large U limit the swapping strength 2κ still causes the reflection. This can be seen from the following analytical result of Eq. (24). However, we would like to point that the resonant transmission may be achieved when the optimal strengths of the two terms are taken. In this work, we introduce the NN interaction V to seek the perfect coherent shift. This mechanism can be seen in the following reduced single-particle Hamiltonian.

Considering the scattering problem without loss of generality, we set the particle $\tilde{b}^\dagger|\text{vac}\rangle$ at the zeroth site and incident the particle $\tilde{a}^\dagger|\text{vac}\rangle$ from $-\infty$ at the beginning. For the scattering process between them within a short duration, the particle $\tilde{b}^\dagger|\text{vac}\rangle$ is static compared to the single particle $\tilde{a}^\dagger|\text{vac}\rangle$. Then the whole scattering process is dominantly governed by

$$\begin{aligned} \mathcal{H}_{\text{eff}}^{\text{U}} = {} & -\kappa \sum_{i=-\infty} \tilde{a}_i^\dagger \tilde{a}_{i+1} - 2\kappa \tilde{b}_{-1}^\dagger \tilde{b}_0 \tilde{a}_0^\dagger \tilde{a}_{-1} + \text{H.c.} \\ & + 2V(\tilde{a}_{-1}^\dagger \tilde{a}_{-1} \tilde{b}_0^\dagger \tilde{b}_0 + \tilde{b}_{-1}^\dagger \tilde{b}_{-1} \tilde{a}_0^\dagger \tilde{a}_0) \\ & + U \tilde{b}_0^\dagger \tilde{b}_0 + U \tilde{b}_{-1}^\dagger \tilde{b}_{-1} \end{aligned} \tag{8}$$

at the condition $|U| \gg |\kappa| \sim |V|$. Here we neglected the terms with κ^2/U and κ^2/V. The swapping process between a single particle and a on-site BP is the key of the coherent shift, which is schematically illustrated in Fig. 1(a). The scattering process is represented in the form

$$\tilde{a}_{-\infty}^\dagger \tilde{b}_0^\dagger |\text{vac}\rangle \rightarrow r \tilde{a}_{-\infty}^\dagger \tilde{b}_0^\dagger |\text{vac}\rangle + t \tilde{a}_{\infty}^\dagger \tilde{b}_{-1}^\dagger |\text{vac}\rangle, \tag{9}$$

where r and t are the reflection and transmission (coherent shift) amplitudes, respectively.

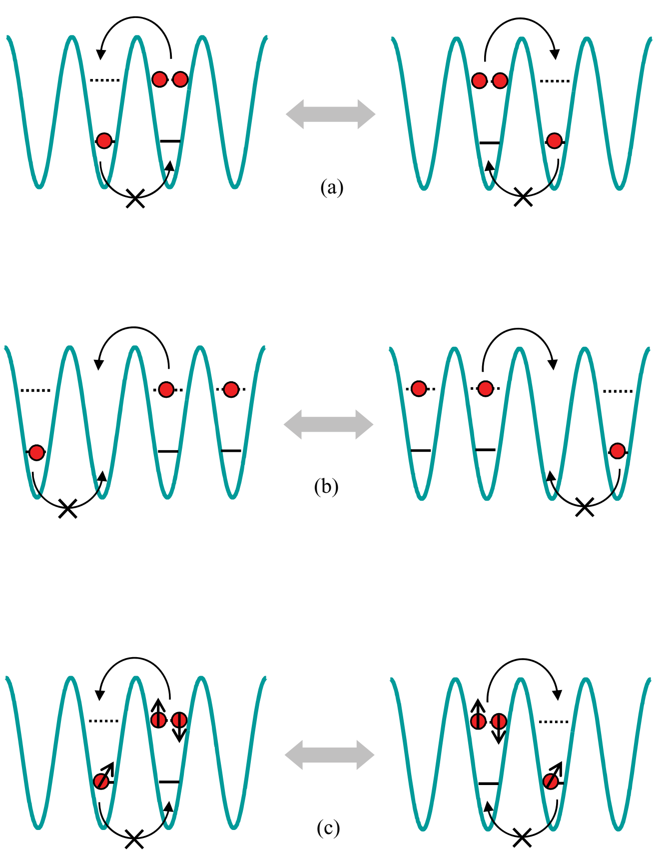

FIG. 1. (Color online) Schematic illustrations of the swapping processes leading to the perfect coherent shift in both Bose and Fermi systems. (a) On-site BP in an extended Bose-Hubbard model. (b) NN BP in an extended Bose-Hubbard model. (c) On-site singlet BP in a simple Fermi-Hubbard model.

In order to investigate the above Hamiltonian Eq. (8), we define a different set of basis $\{|l\rangle_u\}$ as

$$|l\rangle_u \equiv \begin{cases} \tilde{a}_l^\dagger \tilde{b}_0^\dagger |\mathrm{vac}\rangle = \tilde{a}_l^\dagger \tilde{a}_0^{\dagger 2}/\sqrt{2}|\mathrm{vac}\rangle & (l < 0), \\ \tilde{b}_{-1}^\dagger \tilde{a}_l^\dagger |\mathrm{vac}\rangle = \tilde{a}_{-1}^{\dagger 2} \tilde{a}_l^\dagger/\sqrt{2}|\mathrm{vac}\rangle & (l \geqslant 0), \end{cases} \tag{10}$$

and then reduce the two-body problem to a single-particle problem. Actually, acting the Hamiltonian of Eq. (8) or the original Hamiltonian Eq. (1) on the basis (10), we obtain the equivalent single-particle Hamiltonian

$$H_{\mathrm{sp}} = -\kappa \left(\sum_{l=-\infty}^{-2} + \sum_{l=0}^{+\infty} \right) |l\rangle_u \langle l+1| - 2\kappa| - 1\rangle_u \langle 0| + \mathrm{H.c.} \\ + 2V(|-1\rangle_u\langle -1| + |0\rangle_u\langle 0|). \tag{11}$$

The physics of the equivalent Hamiltonian is obvious—it describes a particle in the chain with an embedded impurity. The impurity consists of two neighboring sites with identical on-site potentials $2V$ and a tunneling strength 2κ between them. Obviously, each impurity can lead to nonzero reflection individually. However, when the optimal strengths of V are chosen, total transmission may be realized. In the following, we will investigate this problem with analytical and numerical tools. Figure 2 is a schematic illustration for the equivalent Hamiltonian. Then the scattering process of Eq. (9) can be rewritten as

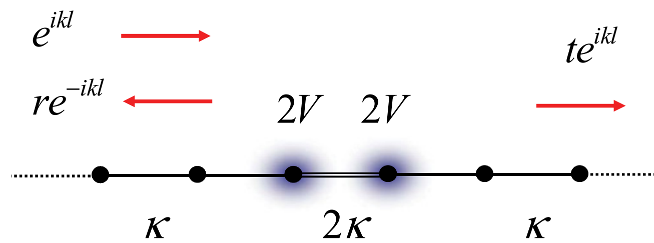

FIG. 2. (Color online) Schematic illustration of the equivalent effective Hamiltonian governs the evolution of a single particle and an on-site BP. It is a chain with an embedded impurity, which consists of two neighboring sites with identical on-site potentials $2V$ and a tunneling strength 2κ between them. The resonant transmission occurs at $V = V_R$, and is equivalent to the perfect coherent shift.

$$a_{-\infty}^\dagger|\mathrm{vac}\rangle \rightarrow r a_{-\infty}^\dagger|\mathrm{vac}\rangle + t a_{\infty}^\dagger|\mathrm{vac}\rangle. \tag{12}$$

The transmission coefficient $|t|^2$ corresponds to the success probability of the coherent shift. For an incident plane wave of momentum k, its expression as a function of k and V can be derived by using the Green's function method [14,15] or the Bethe-ansatz technique [16].

The retarded Green's function of the system of Eq. (11) for an input energy $E = -2\kappa \cos k$ is

$$G^R = \frac{1}{E - H_c - \sum^R}, \tag{13}$$

where H_c is the Hamiltonian of the central system

$$H_c = \begin{pmatrix} 2V & -2\kappa \\ -2\kappa & 2V \end{pmatrix}, \tag{14}$$

and $\sum^R$ denotes the contribution of the half-infinite leads, which can be viewed as an effective Hamiltonian arising from the interaction of the central system with the leads

$$\sum^R = \begin{pmatrix} -\kappa e^{ik} & 0 \\ 0 & -\kappa e^{ik} \end{pmatrix}. \tag{15}$$

The transmission probability is given by

$$|t|^2 = T_{12} = \mathrm{Tr}[\Gamma_1 G^R \Gamma_2 G^A], \tag{16}$$

where the advanced Green's function G^A and $\Gamma_{1,2}$ matrices are

$$G^A = G^{R\dagger}, \quad \Gamma_1 = \begin{pmatrix} 2\kappa \sin k & 0 \\ 0 & 0 \end{pmatrix}, \quad \Gamma_2 = \begin{pmatrix} 0 & 0 \\ 0 & 2\kappa \sin k \end{pmatrix}. \tag{17}$$

Then we can obtain the transmission probability as

$$T_{12} = \frac{16 \sin^2 k}{\prod_{l=-1,1}[4(V/\kappa + l)^2 + 4(V/\kappa + l)\cos k + 1]}. \tag{18}$$

Noting that the transmission coefficient is k dependent, we calculate the resonant transmission or perfect coherent shift. For $T_{12} = 1$, we have the NN coupling constant $V = V_R$, where

$$V_R = \frac{\kappa}{2}(-\cos k \pm \sqrt{\cos^2 k + 3}). \tag{19}$$

It is worth noting that Eq. (19) is available for any k, since V_R is always in the order of κ. In practice, this process can be implemented via a broad wave packet. For the case of $k = \pi/2$, which corresponds to the stablest and fastest wave packet [17], we can generate a unitary swap between an on-site BP and a single particle under the condition $V_R = \pm\sqrt{3}\kappa/2$. In this condition, the k-dependent transmission coefficient $T_{12}(k) = 4\sin^2 k/(4 - \cos^2 k)$ and we notice that $T_{12}(\pi/2) = 1$. Then we get the conclusion that the perfect coherent shift can be achieved in the Bose-Hubbard model with a weak NN interaction and a large U limit.

In order to demonstrate the coherent shift quantitatively and to verify the above analysis, we perform the numerical simulation for a three-particle model H^{B} of Eq. (1) on an N-site chain (N is even). The coherent shift will be simulated via the dynamical process driven by H^{B}. Initially, a BP is located at $(N/2+1)$th site, while a single boson wave packet comes from the left. The initial wave function has the form

$$|\psi(0)\rangle = \frac{1}{\sqrt{2\Omega}} \sum_j e^{-\frac{\alpha^2}{2}(j-N_c)^2 + ik_0 j} a_j^\dagger a_{\frac{N}{2}+1}^{\dagger 2} |\mathrm{vac}\rangle, \tag{20}$$

where k_0, N_c ($N_c \prec N/2$) denote the speed and the initial position of the wave packet of the Gaussian type. Ω is the normalization factor and α controls the width of the packet. As $\alpha \to 0$, the wave packet is reduced to a plane wave with momentum k_0, which is used in the above analytical analysis. We compute the following quantities during the scattering process,

$$\rho_j = \frac{1}{2}\langle a_j^{\dagger 2} a_j^2 - a_j^{\dagger 3} a_j^3 \rangle, (j = N/2, N/2+1), \tag{21}$$

$$n_L = \sum_{j=1}^{N/2} \langle a_j^\dagger a_j - a_j^{\dagger 2} a_j^2 + \frac{1}{2} a_j^{\dagger 3} a_j^3 \rangle, \tag{22}$$

$$n_R = \sum_{j=N/2+1}^{N} \langle a_j^\dagger a_j - a_j^{\dagger 2} a_j^2 + \frac{1}{2} a_j^{\dagger 3} a_j^3 \rangle, \tag{23}$$

where $\langle A \rangle$ denotes the expectation value $\langle \psi(t)|A|\psi(t)\rangle = \langle \psi(0) e^{iH^{\mathrm{B}}t} |A| e^{-iH^{\mathrm{B}}t} \psi(0)\rangle$ at time t. Note that n_L (n_R) denotes the total single-particle number on the left (right) of the BP, while ρ_j denotes the BP number at the jth site. According to the above analysis, for perfect coherent shift, we have $n_L = \rho_{N/2+1} = 1$, $n_R = \rho_{N/2} = 0$ at $t = -\infty$, and $n_L = \rho_{N/2+1} = 0$, $n_R = \rho_{N/2} = 1$ at $t = \infty$. In practice, the simultaneous switches of n_L, $\rho_{N/2+1}$ and n_R, $\rho_{N/2}$ demonstrate the (probably imperfect) coherent shift. We plot $n_{L,R}$ and $\rho_{N/2,N/2+1}$ as a function of time in Figs. 3(a) and 3(b) for a small size system. We consider the incident wave packets with $k_0 = \pi/2$, $N_c = 7$, and $\alpha = 0.5$ and 0.4 for the systems with $N = 26$, $V/\kappa = \sqrt{3}/2$, and $U/\kappa = 30$, 50, and 10^3, respectively. Initially, a BP is located at the 14th site. The transmission probability and the coherent shift efficiency can be obtained from the asymptotic values of n_R and $\rho_{N/2}$, which are labeled on the right-hand side of the figure. The coherent shift of the BP can be demonstrated from the temporal behavior of $\rho_{N/2,N/2+1}$. It shows that the transmission probability (transmitted single-particle number) increases as U becomes large. However, it cannot approach perfect transmission even in the large U limit, which seems differ from our prediction based on Eq. (18). It is due to the

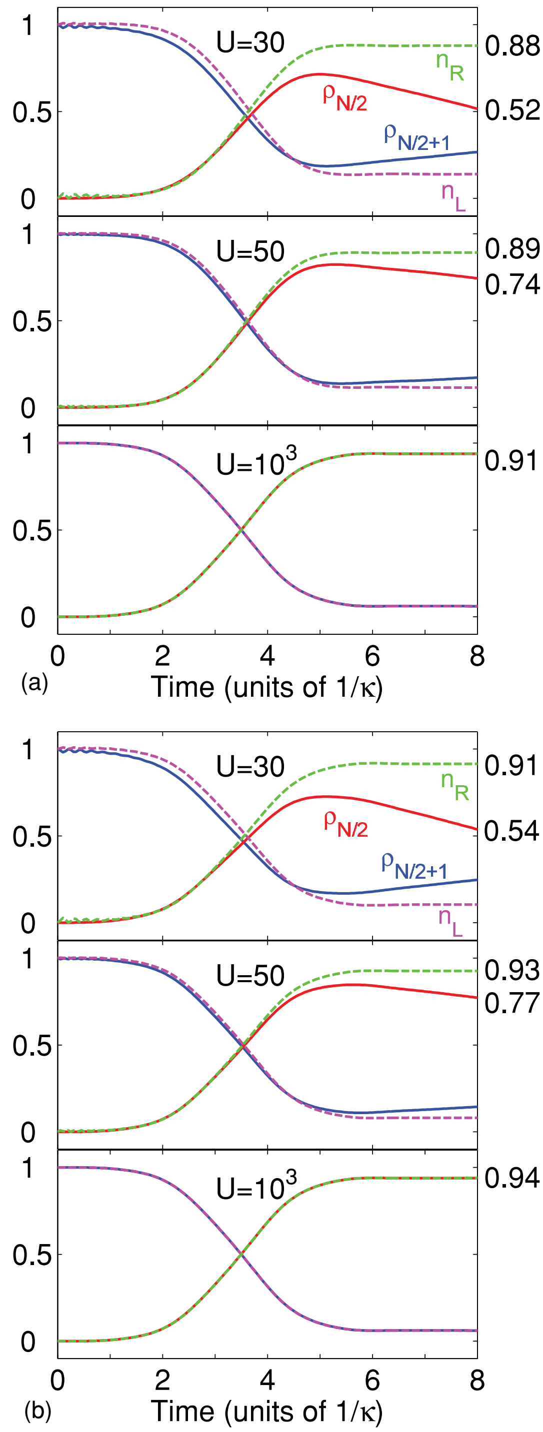

FIG. 3. (Color online) The expectation values of the single-particle and BP numbers, which are defined in Eqs. (21)–(23), as functions of time. The simulation is performed in the 26-site systems with $V/\kappa = \sqrt{3}/2$, $U/\kappa = 30$, 50, and 10^3, respectively. The parameters for the Gaussian wave packets are $k_0 = \pi/2$, $N_c = 7$, and $\alpha = 0.5$ for (a) [0.4 for (b)]. A BP is at the 14th site initially. The dashed lines indicate $n_{L,R}$ (magenta for n_L, green for n_R), while the solid lines indicate $\rho_{N/2,N/2+1}$ (red for $\rho_{N/2}$, blue for $\rho_{N/2+1}$). In each case, the simultaneous switches of solid and dished lines demonstrate the coherent shift. The asymptotic values of $n_{L,R}$, are labeled on the right-hand side of the figure, which reveal the transmission probability and the coherent shift efficiency.

fact that our simulations employ the wave packet instead of the plane wave. One can note that the transmission probability enhances as smaller α is taken. We believe that it will tend to 1 as α approaches zero. Correspondingly, the switch of $\rho_{N/2}$ and $\rho_{N/2+1}$ demonstrates the BP coherent shift. The plots show the influence of relevant parameters to the efficiency of the coherent shift. For the case of $U = 30$, one can see that the right BP number $\rho_{N/2+1}$ starts to decrease from 1 while the left single-particle number n_L remains 1. This shows that the initial BP spreads before the scattering occurs. For large U ($U = 50$, 10^3), the spreading is suppressed. Especially, for $U = 10^3$, $\rho_{N/2}$ can reach 0.91 for $\alpha = 0.5$ (0.94 for $\alpha = 0.4$) after scattering and becomes close to n_R. This demonstrates a good coherent shift of the BP and implies that the perfect coherent shift can be achieved if a sufficiently smaller α is taken.

In the previous work [10], we only consider the simplest Bose-Hubbard model, in which the NN interaction is not included. It has been pointed that a perfect coherent shift cannot be reached [12]. One can also compute the corresponding transmission probability for the simplest Bose-Hubbard model studied in Refs. [10] and [12], by employing the above-mentioned Green's function method. Actually, from Eq. (18), one can get

$$T_{12}(V = 0) = 16\sin^2 k/(9 + 16\sin^2 k) \tag{24}$$

by simply taking $V = 0$. It reaches its maximum 0.64 at $k = \pi/2$, which is in agreement with the result obtained from the computation of the effective Hamiltonian [12]. The switching strength of the BP and the single particle being 2κ are the key reasons for the imperfect coherent shift in the case of $V = 0$.

IV. NN BOUND PAIR IN BOSE SYSTEM

Now we consider another kind of BP in the extended Bose-Hubbard model of Eq. (1) to avoid the reflection caused by the swapping strength being 2κ between the BP and the single particle in a uniform chain. This bound pair is bounded by the NN interaction V, rather than the on-site interaction U. The swapping between the NN BP and the single particle now is κ and becomes the same with a single-particle hopping strength. In a large V limit, $|V|$, $|V-U| \gg |\kappa|$, a pair of hardcore bosons can be bounded by the NN interaction V. This was pointed out by Valiente *et al.* in their work [11]. In such a condition, the dynamics of a single boson and a NN BP can be depicted by the following effective Hamiltonian,

$$\begin{aligned} H_{\text{eff}}^{\text{V}} =& -\kappa \sum_i (a_i^\dagger a_{i+1} + B_i^\dagger B_{i+2} a_{i+3}^\dagger a_i + \text{H.c.}) \\ &+ \left(\frac{\kappa^2}{V} + \frac{2\kappa^2}{V-U}\right) \sum_i (B_i^\dagger B_{i+1} + \text{H.c.}) \\ &- \frac{2\kappa^2}{V} \sum_i (B_i^\dagger B_i a_{i-2}^\dagger a_{i-2} + B_i^\dagger B_i a_{i+3}^\dagger a_{i+3}) \\ &+ \left(V + \frac{2\kappa^2}{V} + \frac{4\kappa^2}{V-U}\right) \sum_i B_i^\dagger B_i, \end{aligned} \tag{25}$$

where the NN pair operator is defined as $B_i^\dagger = a_i^\dagger a_{i+1}^\dagger$. For the scattering process between the NN BP and the single particle within a short duration, it is dominantly governed by the first term, which includes the hopping of a single particle and the swapping between them. The swapping process is schematically illustrated in Fig. 1(b). We consider the scattering problem between a single particle and a NN BP. Initially, a NN BP $B_2^\dagger|\text{vac}\rangle = a_2^\dagger a_3^\dagger|\text{vac}\rangle$ is located at the dimer of sites 2 and 3, while a single particle $a^\dagger|\text{vac}\rangle$ is located at the left. Similarly, we can define a set of basis $\{|l\rangle_v\}$ as

$$|l\rangle_v \equiv \begin{cases} a_l^\dagger B_2^\dagger|\text{vac}\rangle = a_l^\dagger a_2^\dagger a_3^\dagger|\text{vac}\rangle & (l \leqslant 0), \\ B_0^\dagger a_{l+2}^\dagger|\text{vac}\rangle = a_0^\dagger a_1^\dagger a_{l+2}^\dagger|\text{vac}\rangle & (l > 0). \end{cases} \tag{26}$$

Acting the Hamiltonian Eq. (25) on the basis Eq. (26), after neglecting the high-order terms κ^2/V and $\kappa^2/(V-U)$, we obtain a uniform tight-binding chain. Obviously, such a system can realize a perfect coherent shift for any incident single-particle wave with the shift distance being *two lattice spacings*. Comparing to the previous on-site BPs, the perfect coherent shift of the NN BP is k independent.

The corresponding numerical simulation is executed for a three-particle model H^{B} on an N-site chain (N is even); here the BP is bounded by the NN interaction V. The coherent shift will be simulated via the dynamical process driven by H^{B}. Initially, a NN BP is located at the $(N/2+1)$th and $(N/2+2)$th sites, while a single boson wave packet comes from the left. Similarly, the initial wave function has the form

$$|\psi(0)\rangle = \frac{1}{\sqrt{\Omega}} \sum_j e^{-\frac{\alpha^2}{2}(j-N_c)^2 + ik_0 j} a_j^\dagger \left(a_{\frac{N}{2}+1}^\dagger a_{\frac{N}{2}+2}^\dagger\right)|\text{vac}\rangle. \tag{27}$$

We compute the following quantities during the scattering process,

$$\rho_j = \langle n_j n_{j+1}\rangle \quad (j = N/2 \pm 1), \tag{28}$$

$$n_L = \sum_{j=1}^{N/2} \langle \mathfrak{n}_j \rangle, \tag{29}$$

$$n_R = \sum_{j=N/2+1}^{N} \langle \mathfrak{n}_j \rangle, \tag{30}$$

where $\mathfrak{n}_j = a_j^\dagger a_j - a_j^{\dagger 2} a_j^2 + \frac{1}{2} a_j^{\dagger 3} a_j^3 - (n_j n_{j-1} + n_j n_{j+1}) + n_{j-1} n_j n_{j+1}$. Here we take the same denotations as in the last section for simplicity. Note that n_L (n_R) denotes the total single-particle number on the left (right) of the NN BP, while ρ_j denotes the NN BP number at the jth and $(j+1)$th sites. According to the above analysis, for a perfect coherent shift, we have $n_L = \rho_{N/2+1} = 1$, $n_R = \rho_{N/2-1} = 0$ at $t = -\infty$, and $n_L = \rho_{N/2+1} = 0$, $n_R = \rho_{N/2-1} = 1$ at $t = \infty$. In practice, the simultaneous switches of n_L, $\rho_{N/2+1}$ and n_R, $\rho_{N/2-1}$ demonstrate the (probably imperfect) coherent shift. We plot $n_{L,R}$ and $\rho_{N/2-1,N/2+1}$ as functions of time in Fig. 4 for a small size system. We consider the incident wave packets with $k_0 = \pi/2$, $N_c = 7$, $\alpha = 0.4$ for the systems with $N = 26$, $U/\kappa = +\infty$, and $V/\kappa = 30$, 50, and 10^3, respectively. Initially, a NN BP is located at the 14th and 15th sites. The transmission probability and the coherent shift efficiency can be obtained from the asymptotic values of n_R and $\rho_{N/2-1}$, which are labeled on the right-hand side of the figure. It shows that the transmission coefficient (transmitted single-particle number) is always 1. As V goes large, $\rho_{N/2-1}$

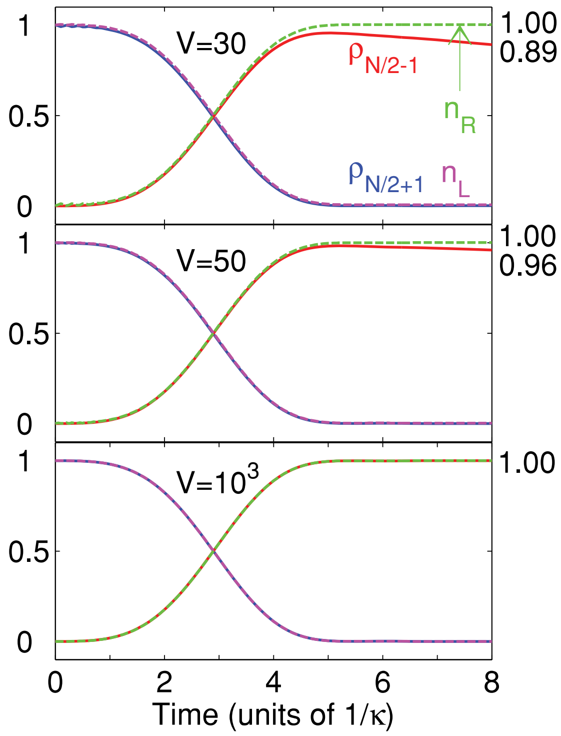

FIG. 4. (Color online) The expectation values of the single-particle and NN BP numbers, which are defined in Eqs. (28)–(30), as functions of time. The simulation is executed in the 26-site systems with $U/\kappa=+\infty$ and $V/\kappa=30$, 50, and 10^3, respectively. The parameters for the Gaussian wave packets are $k_0=\pi/2$, $N_c=7$, and $\alpha=0.4$. A NN BP is at the 14th and 15th sites initially. The dashed lines indicate $n_{L,R}$ (magenta for n_L, green for n_R), while the solid lines indicate $\rho_{N/2-1,N/2+1}$ (red for $\rho_{N/2-1}$, blue for $\rho_{N/2+1}$).

increases and finally approaches 1. The switch of $\rho_{N/2-1}$ and $\rho_{N/2+1}$ demonstrates the NN BP coherent shift. For the case of $V=30$, one can see that the right NN BP number $\rho_{N/2+1}$ starts to decrease from 1 while the left single-particle number n_L remains 1. This shows that the initial NN BP spreads before the scattering occurs. Comparing with the results shown in Fig. 3(b), the coherent shift efficiency is better. For larger V ($V=50$, 10^3), the spread is more suppressed. Especially, for $V=10^3$, $\rho_{N/2-1}$ can reach 1 after scattering and becomes close to n_R. This demonstrates a perfect coherent shift of the NN BP and the switch of $\rho_{N/2-1}$ and $\rho_{N/2+1}$ indicates a *two-lattice-spacing* coherent shift.

V. ON-SITE BOUND PAIR IN FERMI SYSTEM

As pointed out in Ref. [12], the nonzero reflection of a single incident particle in the coherent shift process [10] is attributed to the swapping strength being 2κ rather than κ. Essentially, this arises from the identity of two particles of a BP. Consequently, for a system with a BP consisting of two particles with opposite spins, the unexpected reflection should be avoidable.

Now we turn to the Fermi system. A one-dimensional Fermi-Hubbard Hamiltonian reads

$$H^{\mathrm{F}}=-\kappa\sum_{i,\sigma}(c_{i,\sigma}^{\dagger}c_{i+1,\sigma}+\mathrm{H.c.})+U\sum_{i}n_{i\uparrow}n_{i\downarrow},\qquad(31)$$

where $c_{i,\sigma}^{\dagger}$ is the creation operator of the fermion at the site i with spin $\sigma=\uparrow,\downarrow$ and U is the on-site interaction. Similarly, there also exists a BP state in such a system. Actually, a state in the two-particle Hilbert space with spin zero can be written as of Eq. (2), where we redefine the corresponding basis as

$$\begin{aligned}|\phi_0^k\rangle^{\mathrm{F}}&=\frac{1}{\sqrt{N}}\sum_j e^{ikj}c_{j,\uparrow}^{\dagger}c_{j,\downarrow}^{\dagger}|\mathrm{vac}\rangle,\\ |\phi_r^k\rangle^{\mathrm{F}}&=\frac{1}{\sqrt{2N}}e^{ikr/2}\sum_j e^{ikj}\\ &\quad\times(c_{j,\uparrow}^{\dagger}c_{j+r,\downarrow}^{\dagger}-c_{j,\downarrow}^{\dagger}c_{j+r,\uparrow}^{\dagger})|\mathrm{vac}\rangle.\end{aligned}\qquad(32)$$

Then all the analysis for the formation of a Bose on-site BP can be applied completely on that of a Fermi on-site BP. Besides, in the large U limit, the effective Hamiltonian describing the dynamics of a single particle and a Fermi on-site BP has the form

$$\begin{aligned}H_{\mathrm{eff}}^{\mathrm{F}}&=-\kappa\sum_{i,\sigma}(\tilde{c}_{i,\sigma}^{\dagger}\tilde{c}_{i+1,\sigma}+\tilde{c}_{i,\sigma}^{\dagger}\tilde{c}_{i+1,\sigma}d_{i+1}^{\dagger}d_i+\mathrm{H.c.})\\ &\quad+\frac{2\kappa^2}{U}\sum_i(d_i^{\dagger}d_{i+1}+\mathrm{H.c.})\\ &\quad-\frac{2\kappa^2}{U}\sum_{i,\sigma}\tilde{c}_{i,\sigma}^{\dagger}\tilde{c}_{i,\sigma}(d_{i-1}^{\dagger}d_{i-1}+d_{i+1}^{\dagger}d_{i+1})\\ &\quad+\left(U+\frac{4\kappa^2}{U}\right)\sum_i d_i^{\dagger}d_i,\end{aligned}\qquad(33)$$

where $\tilde{c}_{i,\sigma}=c_{i,\sigma}(1-n_{i,-\sigma})$ is the projected fermion creation operator, and $d_i=c_{i,\downarrow}c_{i,\uparrow}$ is the Fermi on-site BP operator. The projector $(1-n_{i,-\sigma})$ allows to create an electron with spin σ at the site i only if there is no other electron on that site. For the scattering process between $\tilde{c}_{i,\sigma}$ and d_i within a short duration, it is dominantly governed by the first term, which includes the hopping of the single particle and the swapping between them. The swapping process is schematically illustrated in Fig. 1(c). We note that the swapping operation $\tilde{c}_{i,\sigma}^{\dagger}\tilde{c}_{i+1,\sigma}d_{i+1}^{\dagger}d_i$ has the same coupling strength with the term $\tilde{c}_{i,\sigma}^{\dagger}\tilde{c}_{i+1,\sigma}$. This allows the perfect coherent shift. In addition, such a process is independent of the momentum of the incident particle and the spin polarization, since the bound pair is singlet.

In order to demonstrate the coherent shift quantitatively and to verify the above analysis, we perform the numerical simulation for a three-spin model H^{F} of Eq. (31) on an N-site chain (N is even). The coherent shift will be simulated via the dynamical process driven by H^{F}. Initially, a Fermi on-site BP is located at the $(N/2+1)$th site, while a single spin-up wave packet comes from the left. The initial wave function has the form

$$|\psi(0)\rangle=\frac{1}{\sqrt{\Omega}}\sum_j e^{-\frac{\alpha^2}{2}(j-N_c)^2+ik_0j}c_{j,\uparrow}^{\dagger}\left(c_{\frac{N}{2}+1,\uparrow}^{\dagger}c_{\frac{N}{2}+1,\downarrow}^{\dagger}\right)|\mathrm{vac}\rangle,\qquad(34)$$

where k_0, N_c ($N_c\prec N/2$) denote the speed and the initial position of the wave packet of the Gaussian type, respectively. Ω is the normalization factor and α controls the width of the packet. As $\alpha\rightarrow 0$, the wave packet is reduced to the

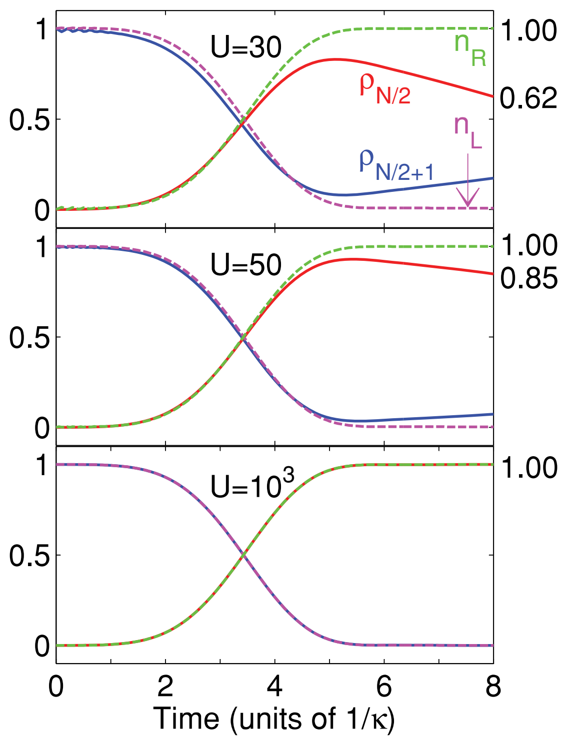

FIG. 5. (Color online) The expectation values of the single spin-up particle and Fermi on-site BP numbers, which are defined in Eqs. (35)–(37), as functions of time. The simulation is performed in the 22-site systems with $U/\kappa = 30$, 50, and 10^3, respectively. The parameters for the Gaussian wave packets are $k_0 = \pi/2$, $N_c = 7$, and $\alpha = 0.4$. A Fermi on-site BP is at the 14th site initially. The dashed lines indicate $n_{L,R}$ (magenta for n_L, green for n_R), while the solid lines indicate $\rho_{N/2,N/2+1}$ (red for $\rho_{N/2}$, blue for $\rho_{N/2+1}$).

plane wave with momentum k_0, which is used in the above analytical analysis. We compute the following quantities during the scattering process,

$$\rho_j = \langle c_{j,\uparrow}^{\dagger} c_{j,\uparrow} c_{j,\downarrow}^{\dagger} c_{j,\downarrow} \rangle \quad (j = N/2, N/2+1), \tag{35}$$

$$n_L = \sum_{j=1}^{N/2} \langle c_{j,\uparrow}^{\dagger} c_{j,\uparrow} - c_{j,\uparrow}^{\dagger} c_{j,\uparrow} c_{j,\downarrow}^{\dagger} c_{j,\downarrow} \rangle, \tag{36}$$

$$n_R = \sum_{j=N/2+1}^{N} \langle c_{j,\uparrow}^{\dagger} c_{j,\uparrow} - c_{j,\uparrow}^{\dagger} c_{j,\uparrow} c_{j,\downarrow}^{\dagger} c_{j,\downarrow} \rangle, \tag{37}$$

where n_L (n_R) denotes the total single spin-up particle number on the left (right) of the Fermi on-site BP, while ρ_j denotes the Fermi on-site BP number at the jth site. According to the above analysis, for a perfect coherent shift, we have $n_L = \rho_{N/2+1} = 1$, $n_R = \rho_{N/2} = 0$ at $t = -\infty$, and $n_L = \rho_{N/2+1} = 0$, $n_R = \rho_{N/2} = 1$ at $t = \infty$. In practice, the simultaneous switches of n_L, $\rho_{N/2+1}$ and n_R, $\rho_{N/2}$ demonstrate the (probably imperfect) coherent shift. We plot $n_{L,R}$ and $\rho_{N/2,N/2+1}$ as functions of time in Fig. 5 for a small size system. We consider the incident wave packets with $k_0 = \pi/2$, $N_c = 7$, and $\alpha = 0.4$ for systems with $N = 22$, $U/\kappa = 30$, 50, and 10^3, respectively. Initially, a Fermi on-site BP is located at the 14th site. The transmission probability and the coherent shift efficiency can be obtained from the asymptotic values of n_R and $\rho_{N/2}$, which are labeled on the right-hand side of the figure. It shows that the transmission coefficient (transmitted single spin-up particle number) is always 1. Correspondingly, the switch of $\rho_{N/2}$ and $\rho_{N/2+1}$ demonstrates the Fermi on-site BP coherent shift. For the case of $U = 30$, one can see that the right Fermi on-site BP number $\rho_{N/2+1}$ starts to decrease from 1 while the left single spin-up particle number n_L remains 1. This shows that the initial Fermi on-site BP spreads before the scattering occurs. For large U ($U = 50$, 10^3), the spreading is suppressed. Especially, for $U = 10^3$, $\rho_{N/2}$ can reach 1 after scattering and becomes close to n_R. This demonstrates a perfect coherent shift of the Fermi on-site BP in a large U limit.

VI. CONCLUSION

In summary, we present three kinds of bound pairs and the corresponding optimal systems, which can avoid unexpected reflection in the coherent shift process. It is shown exactly that the perfect coherent shift can be achieved in simply engineered systems. For a Bose on-site BP, the perfect coherent shift requires a resonant condition which depends on the NN interaction strength and the momentum of the incident single-particle wave packet. For a Bose NN BP and a Fermi on-site BP, the perfect coherent shifts occur for an arbitrary initial state in simple chain systems. We believe that our findings have great potential for future applications.

ACKNOWLEDGMENT

We acknowledge the support of the CNSF (Grants No. 10874091 and No. 2006CB921205).

[1] K. Winkler, G. Thalhammer, F. Lang, R. Grimm, J. H. Denschlag, A. J. Daley, A. Kantian, H. P. Büchler, and P. Zoller, Nature (London) **441**, 853 (2006).

[2] S. M. Mahajan and A. Thyagaraja, J. Phys. A **39**, L667 (2006).

[3] D. Petrosyan, B. Schmidt, J. R. Anglin, and M. Fleischhauer, Phys. Rev. A **76**, 033606 (2007).

[4] C. E. Creffield, Phys. Rev. A **75**, 031607(R) (2007).

[5] A. Kuklov and H. Moritz, Phys. Rev. A **75**, 013616 (2007).

[6] D. Petrosyan, B. Schmidt, J. R. Anglin, and M. Fleischhauer, Phys. Rev. A **76**, 033606 (2007).

[7] S. Zöllner, H.-D. Meyer, and P. Schmelcher, Phys. Rev. Lett. **100**, 040401 (2008).

[8] L. Wang, Y. Hao, and S. Chen, Eur. Phys. J. D **48**, 229 (2008).

[9] M. Valiente and D. Petrosyan, J. Phys. B **41**, 161002 (2008).

[10] L. Jin, B. Chen, and Z. Song, Phys. Rev. A **79**, 032108 (2009).
[11] M. Valiente and D. Petrosyan, J. Phys. B **42**, 121001 (2009).
[12] M. Valiente, D. Petrosyan, and A. Saenz, Phys. Rev. A **81**, 066101 (2010).
[13] L. Jin and Z. Song, New J. Phys. (accepted for publication), e-print arXiv:1004.4770v1.
[14] S. Datta, *Electronic Transport in Mesoscopic Systems* (Cambridge University Press, Cambridge, UK, 1995).
[15] S. Yang, Z. Song, and C. P. Sun, e-print arXiv:0912.0324v1.
[16] L. Jin and Z. Song, Phys. Rev. A **81**, 022107 (2010).
[17] W. Kim, L. Covaci, and F. Marsiglio, Phys. Rev. B **74**, 205120 (2006).